Measurement of *in-vivo* Patella Kinematics Using Motion Analysis and Ultrasound (MAUS)

AP Monk*, M Chen†, S Mellon*, CLMH Gibbons*, DJ Beard*, HS Gill‡ and DW Murray*
*NDORMS, University of Oxford, Windmill Road, Oxford, UK OX3 7HE
†School of Computing and Mathematics, University of Derby, Kedleston Road, Derby, UK DE22 1GB
‡Dept of Mechanical Engineering, University of Bath, Claverton Down, Bath, UK, BA2 7AY

***Abstract*—This paper describes a motion analysis ultrasound system (MAUS) designed for the *in-vivo* study of the kinematics of patellofemoral joints (PFJ) in both normal and replaced knees. This system utilises non-iodising radiation to effectively acquire kinematic data during weight-bearing activities. Validation studies on a phantom established that the measurement accuracy of the system was 1.43 mm. A clinical validation trial is included.**

I. Introduction

Total knee replacement (TKR) is the standard treatment for end-stage osteoarthritis when conservative measures have failed. Despite excellent reported survivorship, the patellofemoral joint is the leading site for complications. It is possible that this might be due to abnormal kinematics. Whilst there is a wealth of data regarding sagittal plane kinematics, previous attempts to study coronal plane patellofemoral kinematics have suffered from methodological drawbacks. Studies involving the use of fluoroscopy, CT and MRI have encountered difficulties with the patella being obscured by the components and/or metal artefact [16] [18].

This paper describes a novel technique for measuring coronal plane kinematics by combining Motion Analysis with UltraSound (MAUS). We also present our two pre-clinical studies on ascertaining the accuracy of the measurement technique.

II. Previous Work

The kinematics of PFJ have been studied both in-vitro and in-vivo. The former relies on the use of cadaveric or post-mortem specimens [1] [13] [19]. During such kinematic assessments of the knee joint, the experimental procedure usually aims to represent simplified physiological loading in order to simulate realistic positions of the femur, tibia and patella. This has traditionally been achieved via the application of load through the quadriceps tendons following intra-medullary fixation of the femur and the tibia to a rig [11] [14].

In-vivo measurements of everyday activities such as squatting, normal gait and stepping activity provide more relevant physiological data [17], as pain is most frequently experienced during these common weight-bearing routines. However, acquiring in-vivo motion data is often complicated by the practicality of imaging the knee anatomy. Planar radiographs and 3D tomography (CT, MRI) can produce detailed images of the knee joint but they impose a high degree of restriction on the range of weight-bearing activities feasible within the confined space. Furthermore, both x-ray and magnetic resonance devices are inappropriate for subjects with prosthetic knee joint. Radiation dosage from x-ray based imaging techniques is also a concern for many clinical practices. Nonetheless, these image modalities have been shown to be successful in measuring PFJ kinematics in native knees [9] [15].

The use of ultrasound for assessing anatomical PFJ abnormalities is well established [2] [10] [12]. The advantages of ultrasound are that it does not involve ionising radiation and can be used to image the knee joint in the presence of metallic prostheses. Previous attempts have been made to quantify coronal plane patella movements during flexion and extension using ultrasound; however these were compromised by measurement errors of up to 6.4 mm (2×SD) due to issues with securing the probe to the leg via bracing [6] [16]. The remainder of this article will focus on discussing the methodology of our ultrasound based motion analysis and its validation.

III. Methods

A. Overview

A multiple camera motion capture system was used to capture images of reflective markers mounted on subjects lower limbs and an ultrasound probe. A spatial mapping between the ultrasound image and the motion capture system was established. Therefore, the ultrasound could be used to determine the locations of the patella and bony landmarks on tibial and femoral segments, during a squat exercise.

The MAUS technique can be geometrically described by a number of coordinate systems in which anatomical landmarks are measured (see Figure 1). Gait was measured in reference to the motion system; whereas the bony landmarks were measured in-vivo in the ultrasound image coordinate system. It is often more desirable to describe measurements in a common coordinate system referred to as the global coordinate system. Since both gait and the ultrasound probe were tracked in the VICON coordinate system, it was designated as the global coordinate frame. The ultimate aim of the system is to transform the ultrasound measurement into the global space, thus unify the gait data with the in-vivo landmark data.

B. Calibration and Tracking of Ultrasound Probe

Ultrasound probe calibration is a process in which the unknown transformation from the image space to the global

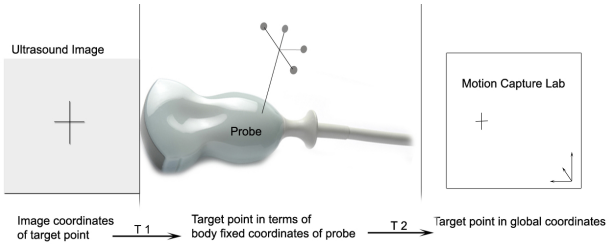

Fig. 1. The spatial relationship between the ultrasound image and the motion capture lab is related by a tracked ultrasound probe.

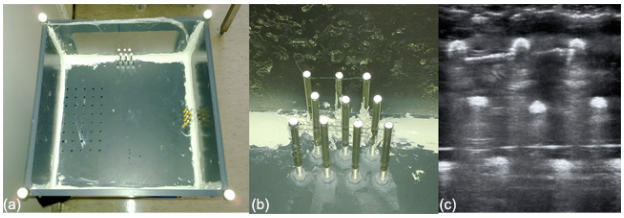

Fig. 2. The point based calibration phantom used in MAUS; (a) Top view of the box containing fiducial markers; (b) Reflective fiducial markers; (c) Ultrasound image of the markers.

coordinate system is calculated. This was achieved by cross-referencing fiducial markers, whose coordinates were known in both global and ultrasound systems. These corresponding coordinates are related to each other by a transformation consisting of a rotation and translation. Hsu et al. discussed and reviewed computational techniques involved in calibrating freehand ultrasound for the purpose of 3D reconstruction [7] [8].

The MAUS system used a calibration phantom consisting of 10 reflective markers for this purpose (see Figure 2a). The markers were fixed within a box consisting of a grid of holes of 2 mm diameter at 10 mm intervals on its base-plate and arranged in a 3-3-4 interlaced formation (Figure 2b). This particular arrangement was adopted to ensure the plane formed by the markers can be unambiguously oriented. Since these markers were reflective and detectable under the optical motion capture system, their global coordinates can be directly localised.

Once the position of each calibration marker was determined, the calibration box remained stationary. The box was then filled with water to allow the propagation of ultrasound. The ultrasound image of fiducial markers was obtained through the surgical membrane at the front of the box (see Figure 2c). Each marker in the image was delineated and its centroid used as its image space position. The position and orientation of the ultrasound probe was simultaneously recorded via a sync trigger when the ultrasound image was captured. This resulted in the following set of known values:

- Coordinates of each calibration marker in the global space $\bar{\mathbf{p}}$.
- Coordinates of each calibration marker in the ultrasound image space $\bar{\mathbf{q}}$.
- Position and orientation of the ultrasound probe in the global space denoted by a 4×4 affine transformation $\mathbf{M}$.

For ultrasound, the relationship between the reconstructed $\bar{\mathbf{p}}'$ and $\bar{\mathbf{q}}$ can be written as:

$$\bar{\mathbf{p}}' = \begin{bmatrix} s_x & 0 & 0 \\ 0 & s_y & 0 \\ 0 & 0 & 1 \end{bmatrix} \mathbf{R}\bar{\mathbf{q}} + \bar{\mathbf{t}} \tag{1}$$

; where s_x and s_y are the image scaling factors. All points in the image space are assumed to be on the xy plane, thus the scaling factor for z is 1. The extrinsic 3×3 rotation matrix $\mathbf{R}$ and translation vector $\bar{\mathbf{t}}$ were solved using the iterative closest point (ICP) method. Further optimisation was performed on all parameters by minimising the cost function (Equation 2) by using the Levenberg-Marquardt algorithm.

$$c(s_x, s_y, \mathbf{R}, \bar{\mathbf{t}}) = \|\bar{\mathbf{p}}' - \bar{\mathbf{p}}\|^2 \tag{2}$$

Since we were interested in tracking the pose of the ultrasound image plane, the transformation $\mathbf{D}$ between the arbitrarily attached tracking sensor and the image plane can be calculated by using Equation 3.

$$\mathbf{D} = \mathbf{M} \begin{bmatrix} \mathbf{R} & \bar{\mathbf{t}} \\ 0 & 1 \end{bmatrix}^{-1} \tag{3}$$

C. Reconstruction of the Lower Limb

The primary purpose of calibrating the ultrasound probe with a stationary phantom is to enable the reconstruction of scanned anatomical landmarks into the global coordinate space. Given an ultrasound scanned landmark obtained at time t, its reconstructed 3D position $\bar{\mathbf{p}}$ was computed by Equation 4;

$$\bar{\mathbf{p}} = \mathbf{M}_t \mathbf{D} \begin{bmatrix} s_x & 0 & 0 \\ 0 & s_y & 0 \\ 0 & 0 & 1 \end{bmatrix} \bar{\mathbf{q}} \tag{4}$$

where denotes the pose of the ultrasound probe at time t; $\bar{\mathbf{q}}$ is the location of a landmark in image space; s_x, s_y and $\mathbf{D}$ are the calibrated parameters.

The lower limb was divided into four orientable segments, i.e. pelvis, femur, tibia and patella. Each segment was constructed by a collection of landmarks including both reconstructed ultrasound landmark and skin-based markers. Figure 3 shows the skin markers attached to a subject. These markers were primarily used to determine the gait stance, e.g. inducing flexion angle.

The reconstruction of the patella position was achieved by using four ultrasound-scanned markers around the peripheral of the patella (see Figure 4).

IV. Results and Discussion

A. Accuracy Assessment and Validation

The accuracy of the measured kinematic data is influenced by the following factors:

1) Systemic accuracy of the motion capture system: The mean results across all sessions of data collection during was 0.28 mm (SD=0.05 mm). The samples were

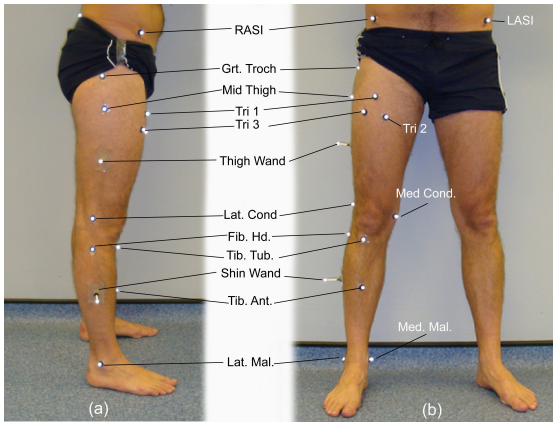

Fig. 3. A reference set of skin markers attached to the subject for gait analysis.

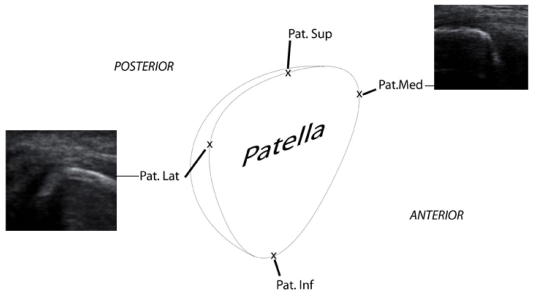

Fig. 4. The ultrasound-scanned landmarks used for defining the geometry of the patella.

VICON Motion Capture System Error		
Sensor	Sample Count	Spatial Error (mm)
1	4166	0.243
2	4095	0.250
3	4733	0.271
4	1004	0.275
5	1994	0.454
6	6400	0.216
7	1330	0.344
8	2277	0.392
9	4332	0.215
10	3776	0.253
11	4167	0.204
	Mean	0.28 mm(SD=0.05)

TABLE I
VICON MOTION CAPTURE SYSTEM ERROR MEASURED FROM EACH SENSOR.

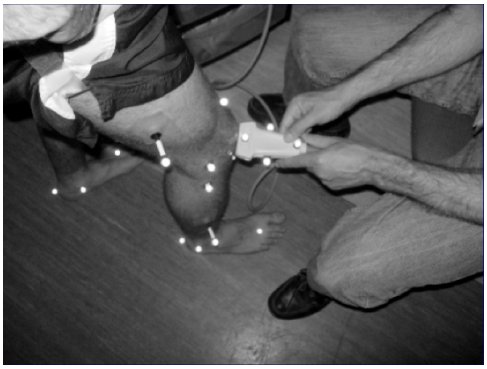

Fig. 5. A clinician using the MAUS system to measure the position of patella of a patient.

RMS errors			
Position	x(mm)	y(mm)	z(mm)
1	0.322	0.774	1.171
	5.439	0.394	1.204
	2.095	1.006	3.836
	0.142	0.085	0.846
2	0.541	0.490	4.664
	0.469	0.040	4.819
	2.045	0.301	6.504
	0.052	0.273	1.593
3	1.051	2.367	1.335
	0.637	2.724	0.741
	0.676	0.324	2.146
	0.835	0.427	1.637
4	2.179	0.435	3.413
	3.162	0.406	2.789
	0.301	0.316	0.812
	0.243	0.256	0.232
Mean	1.262	0.664	2.359
Total Error = 1.428 mm			

TABLE II
ULTRASOUND PROBE CALIBRATION ERRORS MEASURED FROM 16 INDEPENDENT TRAILS IN 4 DIFFERENT SPATIAL POSITIONS.

obtained from each sensor using a calibration wand with known geometric configuration (see Table I).

2) Algorithmic accuracy of the calibration process: The residual error was calculated based on the RMS distances between the computed fiducial markers and their actual positions in the global coordinate system (see Table II). From sixteen independent calibration trials, the overall error was 1.428 mm.
3) Observer measurement error: Two clinicians who were familiar with the operation of ultrasound scanner were recruited as two independent observers. Each observer repeated measurements of the position of 7 anatomical landmarks, in four different positions on four subjects (see Figure 5). Observers using the ultrasound system were able to produce more accurate and consistent kinematic measurements compared to methods based on clamps and skin-markers (see Figure 6).

B. Pre-clinical Validation

The main motivation of implementing this system was to examine the coronal plane PFJ kinematics of both native and replaced knees. The MAUS technique was validated on a cohort of 11 subjects including native and replaced knees. Each subject performed a squatting exercise during the data collection session. The kinematics were analysed at seven discrete flexion angles at full extension, 20, 30, 45, 60 and 90. Our initial observations confirmed the difference in kinematic pattern in native and replaced knees (see Figure 7).

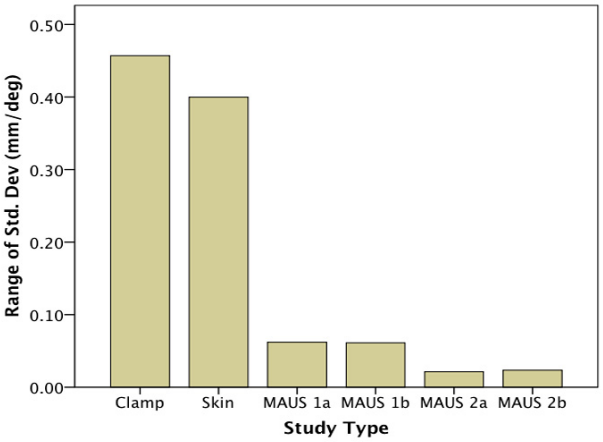

Fig. 6. Inter- and intra-observation study shows accurate and repeatable *in-vivo* measurement of patella displacement versus knee flexion. MAUS demonstrates better accuracy compared to patella clamp [18] and skin movement artefact [3] [4] [5].

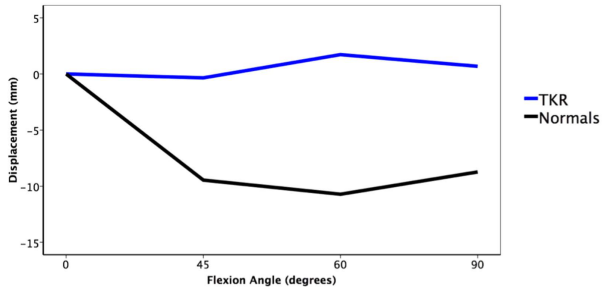

Fig. 7. Mediolateral movements of the patella measured in the coronal plane.

V. Conclusion

This study has demonstrated the implementation and application of an ultrasound based motion analysis technique for in-vivo measuring the motion of the patella in relation to distal femur and proximal tibia. We specifically devised a calibration method using reflective fiducial markers to facilitate the integration with existing motion capture system. The system has been validated both on phantom using fiducial markers and on subjects with native and replaced knees. The 3D reconstruction has enabled clinicians to study the kinematics of PFJ in planes that were restricted in other imaging modalities. A full clinical trial using this measurement technique is currently being conducted.

Currently the reconstruction of ultrasound-scanned landmarks is performed as an offline process. In our future work, this reconstruction algorithm can be systematically integrated with the VICON software system. The integration can lead to a further improvement in the temporal alignment of gait and ultrasound data.

Acknowledgment

The authors would like to thank the gait laboratory at Nuffield Orthopaedic Centre in Oxford for providing the motion capture facility.

References

[1] Y. S. Anouchi, L. A. Whiteside, A. D. Kaiser, and M. T. Milliano, "The effects of axial rotational alignment of the femoral component on knee stability and patellar tracking in total knee arthroplasty demonstrated on autopsy specimens." *Clin Orthop Relat Res*, vol. 187, no. 287, pp. 170–177, 1993.

[2] R. P. Barker, J. C. Lee, and J. C. Healy, "Normal sonographic anatomy of the posterolateral corner of the knee." *ARJ Am J Roentgenol*, vol. 192, no. 1, pp. 73–79, 2009.

[3] A. Cappozzo, F. Catani, A. Leardini, M. G. Benedetti, and U. D. Croce, "Position and orientation in space of bones during movement: experimental artefacts," *Clinical Biomechanics*, vol. 11, pp. 90–100, 1996.

[4] R. M. Ehrig, W. R. Taylor, G. N. Duda, and M. O. Heller, "A survey of formal methods for determining the centre of rotation of ball joints," *J. Biomech.*, vol. 39, pp. 2798–2809, 2006.

[5] S. S. Gamage and J. Lasenby, "New least squares solutions for estimating the average centre of rotation and the axis of rotation," *J. Biomech.*, vol. 35, pp. 87–93, 2002.

[6] L. Herrington, I. McEwan, and J. Thom, "Quantification of patella position by ultrasound scanning and its criterion validity." *Ultrasound Med. Biol.*, vol. 32, no. 12, pp. 1833–1836, 2006.

[7] P. W. Hsu, R. W. Prager, A. H. Gee, and G. M. Treece, "Rapid, easy and reliable calibration for freehand 3d ultrasound," *Ultrasound Med. Biol.*, vol. 32, no. 6, pp. 823–835, 2006.

[8] P. W. Hsu, G. M. Treece, R. W. Prager, N. E. Houghton, and A. H. Gee, "Comparison of freehand 3-d ultrasound calibration techniques using a stylus," *Ultrasound Med. Biol.*, vol. 34, no. 10, pp. 1610–1621, 2008.

[9] F. Iranpour, A. M. Merican, F. R. Baena, J. P. Cobb, and A. A. Amis, "Patellofemoral joint kinematics: the circular path of the patella around the trochlear axis," *J. Orthop. Res.*, vol. 28, no. 5, pp. 589–594, 2010.

[10] F. W. Joshi and R. P. Heatley, "Imaging patellofemoral joint using ultrasound: a preliminary report. a comparison between normal subjects and patients with patellar maltracking," *Knee*, vol. 5, pp. 129–135, 1998.

[11] T. Luyckx, K. Didden, H. Vandenneucker, L. Labey, B. Innocenti, and J. Bellemans, "Is there a biomechanical explanation for anterior knee pain in patients with patella alta? influence of patellar height on patellofemoral contact force, contact area and contact pressure," *J. Bone Joint Surg. Br.*, vol. 91, no. 3, pp. 344–350, 2009.

[12] C. Nofsinger and J. G. Konin, "Diagnostic ultrasound in sports medicine: current concepts and advances," *Sports Med Arthrosc*, vol. 17, no. 1, pp. 25–30, 2009.

[13] S. Ostermeier, O. Buhrmester, C. Hurschler, and C. Stukenborg-Colsman, "Dynamic in vitro measurement of patellar movement after total knee arthroplasty: an in vitro study," *BMC Musculoskeletal Disorders*, vol. 6, no. 30, 2005.

[14] A. J. Price, P. T. Oppold, D. W. Murray, and A. B. Zavatsky, "Simultaneous in vitro measurement of patellofemoral kinematics and forces following oxford medial unicompartmental knee replacement," *J. Bone Joint Surg. Br.*, vol. 88, no. 12, pp. 1591–1595, 2006.

[15] J. M. Scarvell, P. Smith, K. M. Refshauge, H. R. Galloway, and K. R. Woods, "Does anterior cruciate ligament reconstruction restore normal knee kinematics?: A prospective mri analysis over two years," *J. Bone Joint Surg. Br.*, vol. 88, no. 3, pp. 324–30, 2006.

[16] Y. F. Shih, A. M. Bull, A. H. McGregor, and A. A. Amis, "Active patellar tracking measurement: a novel device using ultrasound," *Am. J. Sports Med.*, vol. 32, no. 5, pp. 1209–1217, 2004.

[17] A. von Porat, M. Henriksson, E. Holmstrom, and E. M. Roos, "Knee kinematics and kinetics in former soccer players with a 16-year-old acl injury - the effects of twelve weeks of knee-specific training," *BMC Musculoskeletal Disorders*, vol. 8, no. 35, 2007.

[18] N. A. Wilson, J. M. Press, J. L. Koh, and R. W. Hendrix, "In vivo noninvasive evaluation of abnormal patellar tracking during squatting in patients with patellofemoral pain," *JBJS (Am)*, vol. 91, no. 3, pp. 558–566, 2009.

[19] A. B. Zavatsky, "A kinematic-freedom analysis of flexed-knee-stance testing rig," *J. Biomech.*, vol. 30, no. 3, pp. 277–280, 1997.